Driving Mechanism of SOL Plasma Flow and Effects on the Divertor Performance in JT-60U

N. Asakura 1), H. Takenaga 1), S. Sakurai 1), G.D. Porter 2), T.D. Rognlien 2), M.E. Rensink 2), O. Naito 1), K. Shimizu 1), K. Itami 1), S. Higashijima 1), T. Nakano 1), H. Kubo 1), Y. Koide 1), Y. Sakamoto 1), T. Takizuka 1), A.V. Chankin 1), S. Konoshima 1), and the JT-60 Team

1) Japan Atomic Energy Research Institute, Naka-machi, Naka-gun, Ibaraki 311-0193, Japan
2) Lawrence Livermore National Laboratory, P.O.Box 808, Livermore , CA 94550, USA

e-mail: asakuran@fusion.naka.jaeri.go.jp

Abstract. The measurements of the SOL flow and plasma profiles both at the high-field-side (HFS) and low-field-side (LFS), for the first time, identified the SOL flow pattern and its driving mechanism. "Flow reversal" was found near the HFS and LFS separatrix of the main plasma for the ion ∇B drift direction towards the divertor. Radial profiles of the SOL flow were similar to those calculated numerically using the UEDGE code with the plasma drifts included although Mach numbers in measurements were greater than those obtained numerically. Particle fluxes towards the HFS and LFS divertors produced by the parallel SOL flow and $\boldsymbol{E_r xB}$ drift flow were evaluated. The particle flux for the case of intense gas puff and divertor pump (puff and pump) was investigated, and it was found that both the Mach number and collisionality were enhanced, in particular, at HFS. Drift flux in the private flux region was also evaluated, and important physics issues for the divertor design and operation, such as in-out asymmetries of the heat and particle fluxes, and control of impurity ions were investigated.

1. Introduction

The scrape-off layer (SOL) flow plays an important role in the plasma transport along the field lines. Parallel SOL flow is expected to increase with an intense gas puff and divertor pump (puff and pump), which is proposed to improve impurity shielding from the core plasma. On the other hand, the SOL flow away from the LFS divertor, "flow reversal" (opposite to what one expects from a simple picture of the plasma flow), has been generally observed at various locations around the plasma edge, in particular, for the ion ∇B drift direction towards the divertor [1-4]. Recently, mechanisms producing parallel SOL flow, resulting from the poloidal variation of plasma drift velocity were investigated [5,6]. Drift flow in the private flux region was proposed as a candidate mechanism to produce in-out asymmetry in divertor particle flux [7,8]. Quantitative evaluation of the drift effects should be established in order to control the SOL and divertor plasmas in magnetic configurations relevant to a tokamak reactor.

Determination of the SOL flow pattern has been recently advanced in JT-60U experiments. Reciprocating Mach probes were installed at the high-field-side (HFS) baffle, low-field-side (LFS) midplane and just below the X-point (Fig.1). SOL flow pattern is shown in Sec. 2. It is compared to UEDGE simulation results with the plasma drifts included in Sec. 3. SOL particle fluxes towards the HFS and LFS divertors are, for the first time, evaluated from components of the parallel SOL flow and perpendicular E_rxB drift flow. Important physics issues for the divertor design and operation: in-out asymmetry in the ion flux and impurity control by puff and pump, are discussed in Sec. 4 and 5. Summary and conclusions are given in Sec. 6.

2. SOL Flow Measurements at HFS and LFS

Profiles of ion saturation currents at the electron- and ion-drift sides, $j_s^{e\text{-}s}$ and $j_s^{i\text{-}s}$, electron

temperatures, $T_e^{e\text{-}s}$ and $T_e^{i\text{-}s}$, and floating potential, V_f, are measured with spatial resolution of 1-2 mm. The direction of the plasma flow along the field lines and the Mach number are deduced from the ratio of $j_s^{e\text{-}s}$ and $j_s^{i\text{-}s}$, using Hutchinson's formula [9]: $M = 0.35 ln(j_s^{i\text{-}s}/j_s^{e\text{-}s})$, where positive and negative values show the direction towards the LFS and HFS divertors, respectively. Plasma potential, V_p, and radial electric field, E_r, are calculated from a sheath model ($V_p = V_f + 2.75T_e$) and its differentiation. Parameters of the L-mode discharge, I_p=1.6MA, B_t=3.3T, q_{95}=3.5 and P_{NBI}=4.3MW, are fixed. Main plasma density, $\bar{n}_e$, is maintained during probe measurements, and it changes from 1.2×10^{19} to 3.9×10^{19} m^{-3} ($\bar{n}_e/n^{GW}$ =0.23 – 0.73, where n^{GW} =5.2×10^{19} m^{-3}) on a shot-by-shot basis for normal ion ∇B drift direction.

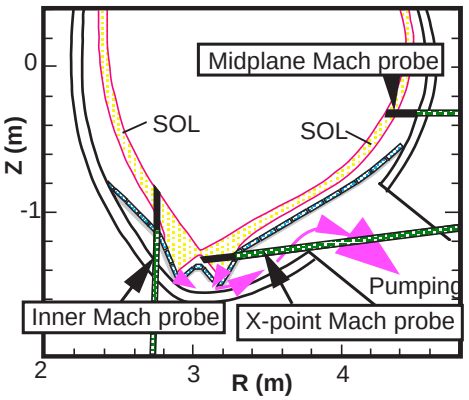

FIG. 1. Profiles of j_s, T_e, V_f and SOL flow along black lines are measured with three reciprocating Mach probes at HFS baffle, LFS midplane, and below X-point.

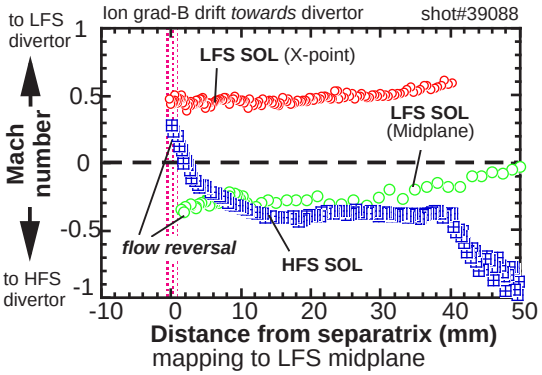

FIG. 2. Profiles of Mach numbers measured by reciprocating Mach probes (at LFS midplane, near X-point and above HFS baffle) for ion grad-B direction towards the divertor.

Both the ion ∇B drift direction and $\bar{n}_e$ were found to affect the plasma flow velocity [6,10]. Profiles of the Mach number at the three locations are shown in Fig. 2 for the ion ∇B drift direction towards the divertor and relatively low $\bar{n}_e$=$1.6\times10^{19}m^{-3}$. Three profiles are mapped to the LFS midplane, and the data in the private flux region are not plotted. For the midplane radius (r_{mid}) less or greater than 4 cm, field lines are connected to the divertor plate and baffle, respectively. Results of the LFS flow profiles show that flow reversal occurs near the separatrix of the main plasma with M = -0.4. The flow reversal gradually reduces at the outer flux surfaces, whereas fast SOL flow (M~ 0.5) towards the LFS divertor is observed below the X-point.

Characteristics of HFS SOL flow change near the separatrix. The SOL flow away from the HFS divertor with $|M|$ = 0.1-0.2 is found at and just outside the separatrix, and width of the flow reversal (r_{mid} ~0.4 cm) is narrower than that observed LFS midplane (r_{mid} < 5cm). The Mach numbers of the flow reversal decrease gradually with increasing $\bar{n}_e$. On the other hand, at the outer flux surfaces (1 < r_{mid} <4cm), subsonic SOL flow towards the HFS divertor (M ~ -0.5) is produced. Mach numbers are similar both at LFS midplane and HFS. Parallel SOL flow may be driven from LFS to HFS on the outer flux surfaces. The Mach numbers increase with $\bar{n}_e$. Particle flux towards the HFS divertor, which is produced by the SOL flow ($n_i V_{//}$) and is represented by $n_i M C_s \sim M j_s/e$, is also enhanced. Particle flux towards the divertor is investigated in Sec. 4.

For the ion ∇B drift direction away from the divertor, SOL flow towards LFS divertor is observed both at LFS midplane and near X-point. The SOL flow at HFS is towards the HFS divertor. All Mach numbers near the separatrix are small ($|M|$ = 0.2-0.3). From these observations in opposite ∇B drift configurations, one can conclude that the SOL flow near the

separatrix of the main plasma edge is driven against the ∇B drift direction. A large influence of the plasma drifts is expected.

3. SOL Plasma Simulation With Drift Effects

Two-dimensional plasma flow pattern was investigated in the toroidal plasma and divertor geometries. Drift effects such as $\boldsymbol{E}$x$\boldsymbol{B}$, $\boldsymbol{B}$x$\boldsymbol{\nabla B}$ and diamagnetic drifts have been included in the simulation code of the plasma fluid models, UEDGE [11]. At this stage, plasma calculation mesh covers the edge and SOL area at the LFS midplain radius of $-3<r_{mid}<5$cm. Constant diffusion coefficients, $\chi_i = \chi_e = 1$ m^{2}s^{-1} and $D = 0.25$ m^{2}s^{-1} over the SOL area, are used to reproduce the measured T_e and n_e profiles at LFS midplane.

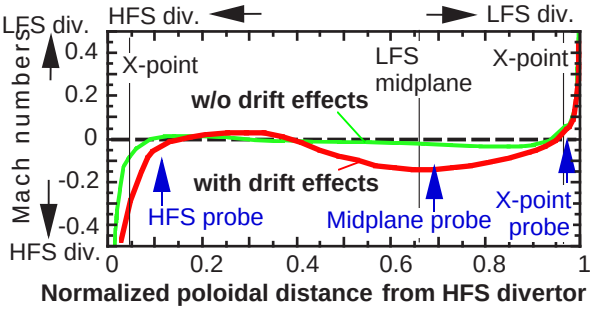

FIG. 3. Mach numbers at r_{mid} = 0.5cm as a function of normalized poloidal distance from HFS divertor. Cases with and without including drift effects are shown. Mach probe locations are shown by arrows.

Figure 3 shows Mach numbers of the parallel SOL flow along the normalized poloidal distance from HFS target to LFS target at r_{mid}=0.6 cm. Here, the calculation with including small drift effects of 55% in iterations is also shown. It is found that the SOL flow towards the HFS divertor, i.e. flow reversal, is produced at LFS SOL, while the SOL flow towards the LFS divertor is seen near the X-point. With increasing drift effects, Mach numbers of the flow reversal increase (in particular, at LFS SOL midplane). Simulation results reveal that the flow reversal is mainly caused by the ion $\boldsymbol{B}$x$\boldsymbol{\nabla B}$ drift, which increases the ion pressure downward. On the other hand, the Mach number at the X-point does not change near the separatrix at relatively low $\bar{n}_e$.

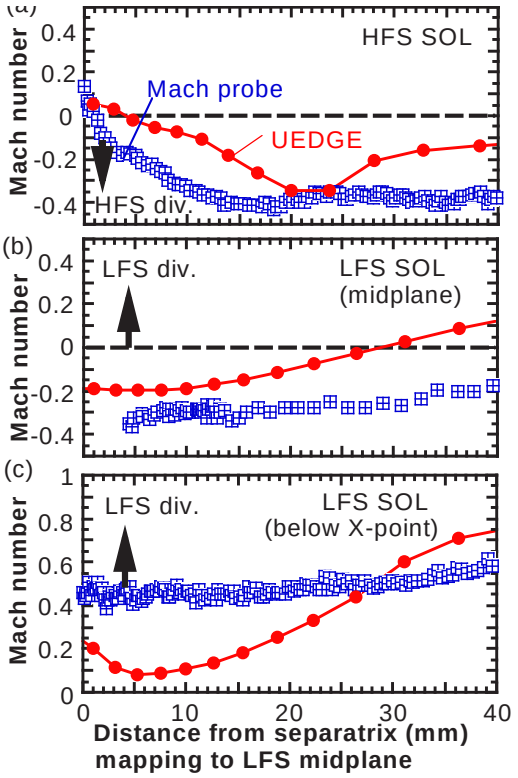

FIG.4. Numerical (with drift effects) and experimental Mach number profiles (a) above HFS baffle, (b) at LFS midplane and (c) near the X-point (LFS SOL).

Calculated SOL flow profiles are compared to the measured ones as shown in Fig. 4 [12]. At the LFS midplane, the flow reversal near the separatrix ($|M|$ ~0.2) is comparable to the measurement ($|M|$ = 0.3-0.4). The calculated SOL flow at the outer flux surfaces (r_{mid} > 3 cm) is towards the LFS divertor: the width of the flow reversal is narrow, while it is observed at further outer radius (r_{mid} > 5 cm) in the experiment. Neutral flux from the first wall is larger in experiments, which is not modeled consistently to reproduce the D_α brightness profile. This influence should be simulated in order to understand radial diffusion of the SOL plasma as well as parallel flow pattern.

Calculated Mach numbers above the HFS baffle and near the X-point increase towards the divertor when the drift effects are included. At HFS SOL, the Mach numbers at separatrix and $r_{mid} \sim 2$ cm are comparable to the measurements, but those within $0< r_{mid}<2$ cm are smaller. On the other hand, near the X-point of LFS, the Mach numbers at $r_{mid} < 2$ cm (including separatrix) are small compared to the measurements ($|M| \sim 0.4$). Mechanism for the subsonic flow in experiments is not understood yet. It could be caused by the fact that distributions of impurity ion densities are not well reproduced to simulate the experimental radiation profile in the divertor. However, near the separatrix, influences of the subsonic flow on net particle flux towards the divertor are relatively small since particle flux caused by the drift flow is larger.

4. Particle Fluxes Towards HFS and LFS Divertors

In this section, net particle fluxes towards the HFS and LFS divertors are investigated [13]. Components of parallel SOL flow ($n_iV_{//}$) and drift flow (n_iV_{drift}) to the particle flux towards the divertor are described as $n_iV_{//}\Theta$ and $n_iV_{drift}\Phi$, respectively. Here, $\Theta = B_p/B_{//}$ varies in torus and $\Phi = B_t/B_{//}$ (~1). Both components change with increasing $\bar{n}_e$. At the same time, large E_rxB drift flow in the private flux region influences the in-out asymmetry in the divertor ion flux [6]. Distributions of the parallel and drift flows upstream of the HFS and LFS divertors and in the private flux region are for the first time established enabling one to understand the particle transport in SOL and divertor.

4.1 Parallel SOL Flow and *Ex*B Drift Flow

Poloidal components of particle flux densities: parallel SOL flow ($n_iV_{//}\Theta$) and E_rxB drift flow ($n_iV_{drift}^{ExB}\Phi$) are shown in Fig.5 for the ion ∇B drift direction towards the divertor. Here, $n_i=n_e$ is assumed. Drift flow has a positive value, which produces particle fluxes away from and towards the divertor at HFS and LFS, respectively. The diamagnetic flow ($n_iV_{drift}^{dia}$) does not constitute the particle flux onto the divertor and is not shown. At the HFS and LFS, poloidal flux density of the drift flow is dominant near the separatrix (r_{mid} <0.4cm). Poloidal components of particle flux density in the private flux region are shown in Fig. 5(b), which is produced by negative E_r in the private plasma under the attached divertor condition. The E_rxB drift flux is very large and it contributes to particle transport from LFS to HFS divertor.

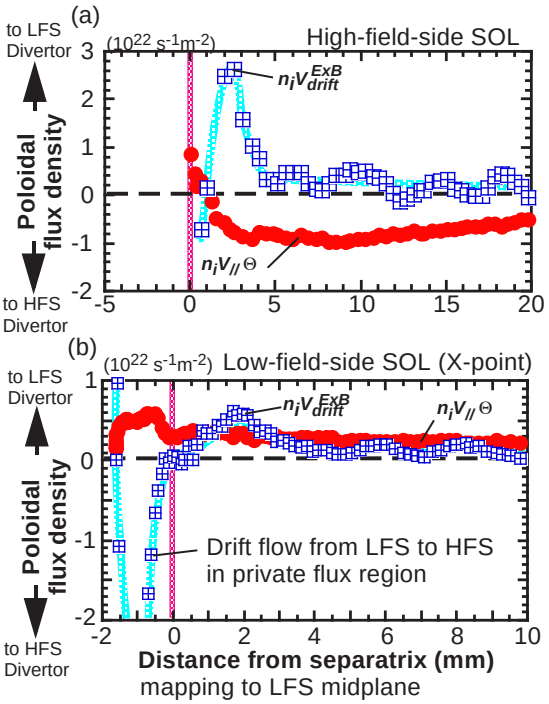

FIG. 5. Components of the poloidal fluxes produced by parallel SOL flow ($n_iV_{//}\Theta$) and E_rxB drift flow ($n_iV_{drift}^{ExB}$), (a) for HFS, and (b) for LFS.

In the detached divertor, negative E_r appears near the boundary of detached and attached plasmas in the common flux region. This E_rxB drift would produce particle flux away from the LFS divertor to the X-point. On the other hand, parallel SOL flow towards the LFS divertor increases up to the sonic level since the ionization front moving from the target plate to the X-

point [4]. The net particle flux is carried towards the LFS divertor.

4.2 Influence of *ExB* Drift on Particle Flux

Influences of the drift flow on total particle fluxes, Γ_p^{HFS} and Γ_p^{LFS}, are investigated. Γ_p^{HFS} and Γ_p^{LFS} are calculated by integrating $n_i V_{//}\Theta$ and $n_i V_{drift}^{ExB}\Phi$ across the SOL along the probe scan from the separatrix (r=0) to the most outer radius ($r=r_{div}$), where field line is connected to the divertor, as follows,

$$\Gamma_p^{HFS/LFS} = \int_0^{r_{div}} 2\pi R n_i [V_{//}\Theta + V_{drift}^{ExB}\Phi]\nabla\varphi \cdot dr \ , \qquad (1)$$

where positive value shows particle flux towards the LFS divertor. Figure 6 shows $|\Gamma_p^{HFS}|$ and Γ_p^{LFS}, and the ratio of E_rxB drift flux to parallel flux as a function of $\bar{n}_e/n^{GW}$. Equation (1) is written as $\Gamma_p^{HFS/LFS} = \Gamma_{p,//}^{HFS/LFS} + \Gamma_{p,drift}^{HFS/LFS}$, where $\Gamma_{p,//}^{HFS}$ and $\Gamma_{p,//}^{LFS}$ have negative and positive values, respectively. Total particle flux at the private flux region, Γ_p^{Prv}, is calculated from Eq.(1), where two components are integrated in the private flux region (-2 < r < 0 cm).

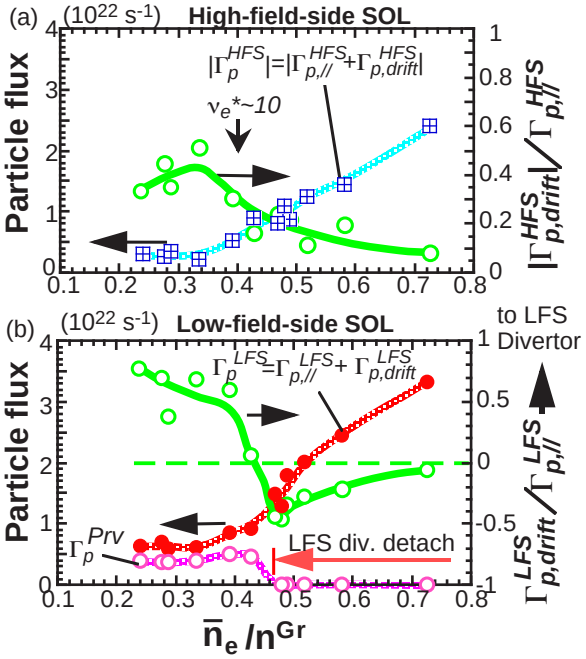

FIG. 6. Net poloidal fluxes towards divertors, Γ_p^{HFS} and Γ_p^{LFS}, and ratio of drift flux to parallel flux, $\Gamma_{p,drift}/\Gamma_{p,//}$, as a function of n_e: (a) for HFS and (b) for LFS near X-point. Drift flux from LFS to HFS, Γ_p^{Prv}, is also shown.

At low $\bar{n}_e$ ($\bar{n}_e/n^{GW}$ =0.24–0.34), $\Gamma_{p,//}^{HFS}$ of -(3.0-4.0)x10^{21} s^{-1} is larger than $\Gamma_{p,drift}^{HFS}$ of (0.9-2.1)x10^{21} s^{-1}. $\Gamma_{p,drift}^{HFS}$ is 30-50% of $|\Gamma_{p,//}^{HFS}|$. Thus, the direction of Γ_p^{HFS} is towards the HFS divertor, and Γ_p^{HFS} is -(1.5-2.5)x10^{21} s^{-1}. On the other hand, $\Gamma_{p,//}^{LFS}$ and $\Gamma_{p,drift}^{LFS}$ are (3.0-4.0)x10^{21} and (1.6-2.9)x10^{21} s^{-1}, respectively. $\Gamma_{p,drift}^{LFS}$ corresponds to 45-80% of $\Gamma_{p,//}^{LFS}$, and Γ_p^{LFS} is (5.9-7.0)x10^{21} s^{-1}. As a result, Γ_p^{LFS} is larger than Γ_p^{HFS}, and the asymmetry is produced mostly by the drift flow in SOL. On the other hand, Γ_p^{Prv} of -(3.7-3.9)x10^{21} s^{-1} is large, and it should contribute to in-out asymmetry in the divertor ion flux.

When the detachment occurs at LFS divertor, however, Γ_p^{Prv} decreases to zero. At the same time, with increasing $\bar{n}_e$, both $|\Gamma_{p,//}^{HFS}|$ and $\Gamma_{p,//}^{LFS}$ increase largely and become dominant in particle transport towards the divertor. Here, $\Gamma_{p,drift}^{LFS}$ changes the direction, as mentioned in Sec. 4.1.

4.3 In-Out Asymmetry in Divertor Ion Flux

Influences of Γ_p^{HFS}, Γ_p^{LFS} and Γ_p^{Prv} on in-out asymmetry in the divertor ion flux are discussed. We make the following assumption: a part of Γ_p^{LFS} is exhausted into the private flux region by diffusion and radial drifts before reaching the target plate: such particle flux would be comparable to $|\Gamma_p^{Prv}|$. Total particle fluxes towards the HFS and LFS divertors are estimated as $\Gamma_p^{HFS}+\Gamma_p^{Prv}$ and $\Gamma_p^{LFS}-|\Gamma_p^{Prv}|$, respectively. $|\Gamma_p^{HFS}+\Gamma_p^{Prv}|$ and $\Gamma_p^{LFS}-|\Gamma_p^{Prv}|$ are shown in Fig. 7 as a

function of $\bar{n}_e/n^{GW}$. For the attached divertor conditions ($\bar{n}_e/n^{GW}$ =0.24 – 0.45), $|\Gamma_p^{HFS}+\Gamma_p^{Prv}|$ of (5.4-12.6)x10^{21}s^{-1}is a factor of 2-3 larger than Γ_p^{LFS} –$|\Gamma_p^{Prv}|$ of (2.2-4.4)x10^{21}s^{-1}. Large contribution of Γ_p^{Prv} to the HFS-enhanced asymmetry in the divertor ion flux is determined.

When the detachment occurs at the LFS divertor at $\bar{n}_e/n^{GW}$ > 0.46, Γ_p^{Prv} disappears and net particle fluxes towards the HFS and LFS divertors are described as Γ_p^{HFS} ($\sim\Gamma_{p,//}^{HFS}$) and Γ_p^{LFS} ($\sim\Gamma_{p,//}^{LFS}$), respectively. At the same time, $\Gamma_{p,//}^{LFS}$ becomes larger than $\Gamma_{p,//}^{HFS}$. As a result, Γ_p^{LFS} becomes a factor of 1.3-1.8 larger than Γ_p^{HFS}. The asymmetry in Γ_p is small compared to that in the attached divertor. Similar HFS-enhanced asymmetries in the particle recycling and neutral pressure have been generally observed [10]. When the divertor detachment occurs such asymmetries become small and reversed. These characteristics of the particle transport in the divertor are determined by changes in Γ_p^{HFS}, Γ_p^{LFS} and Γ_p^{Prv}.

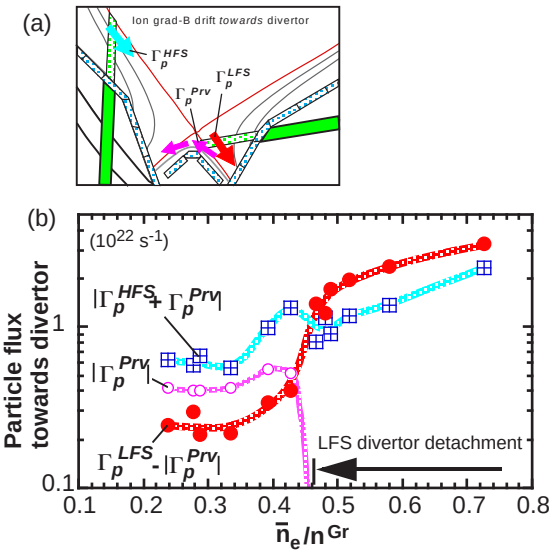

FIG. 7. (a) Directions of particle fluxes are illustrated at HFS, LFS and private flux region. (b) Particle fluxes towards the HFS and LFS divertors are shown as $|\Gamma_p^{HFS}+\Gamma_p^{Prv}|$ and $\Gamma_p^{LFS}-|\Gamma_p^{Prv}|$, respectively.

Contributions of drift effects to the particle transport would be an important question for the divertor design and operations in tokamak reactor such as ITER. Although the high density plasma ($\bar{n}_e/n^{GW}$~0.85) is sustained, collisionality of the SOL plasma is relatively low (ν_e^* = L_{cl}/λ_e ~5-10) since T_e at separatrix (~150 eV) would be high at n_e ~3.5x10^{19} m^{-3}. Relatively large E_r is expected in such low ν_e^*, which corresponds to database at $\bar{n}_e/n^{GW}$~0.4 in Fig.6. Then, $\Gamma_{p,drift}^{HFS}/|\Gamma_{p,//}^{HFS}|$ of ~30% and $\Gamma_{p,drift}^{LFS}/\Gamma_{p,//}^{LFS}$ of ~60% would be anticipated. At the same time, E_rxB drift flow in the private flux region is expected since the divertor detachment is localized near the strike-points: private plasma below the X-point is attached. Particle flux towards the divertor would be influenced by these drifts, and a design work with including these drifts will be useful to optimize the divertor and pump geometries.

5. Effect of Gas Puff Location on SOL Flow

SOL flow pattern is modified depending on the gas puff location, and a technique of the puff and pump was demonstrated to exhaust impurity ions (helium, neon and carbon) from the core plasma [14,15]. However, the SOL flow pattern has not been determined experimentally. The SOL plasma flow was investigated during strong gas puff from the plasma top ("main puff") and divertor ("divertor puff") as shown in Fig.8(a). Mach probes locations are downstream and upstream from the main puff and divertor puff locations, respectively. Constant puff rate is kept during the measurements under the attached divertor condition, and it changes from 20 to 60 Pam^{3}s^{-1} (Γ_{puff} = 1.1-3.2x10^{22} Atoms s^{-1}) on a shot-by-shot basis. Hydrogen L-mode plasma with normal ion ∇B drift direction was used in these experiments.

Profiles of M and n_e are compared for the two cases, where $\bar{n}_e$ are comparable, (2.6-2.7)x10^{19} m^{-3} ($\bar{n}_e/n^{GW}$~ 0.52). For the main puff, enhancements of M and n_e are observed both at HFS and LFS, compared to those for the divertor puff. At HFS, M increases by 20% in the wide region between the separatrix and the outer flux surfaces, and $\bar{n}_e$ also increases by 20-50%. As a result, parallel flux density component ($n_iV_{//}\Theta$) increases as shown in Fig.8 (b). On the other hand, at LFS near the X-point, an increase in M (less than 25%) is observed only at $1<r_{mid}<2$cm, while n_e is comparable. Thus, small increase in $n_iV_{//}\Theta$ is seen only at the outer flux surfaces as shown in Fig.8 (c).

Total parallel flux components, $\Gamma_{p,//}^{HFS}$ and $\Gamma_{p,//}^{LFS}$, which are dominant in the particle transport, are compared between the main puff and the divertor puff. $\Gamma_{p,//}^{HFS}$ is shown in Fig.9. For the main gas puff, large enhancement of $\Gamma_{p,//}^{HFS}$ (a factor of 1.5-2) is found, while $\Gamma_{p,//}^{LFS}$ is 1.1-1.3 times larger. These results suggest that the bulk of the SOL plasma generated by the main puff is brought towards the HFS divertor. This SOL flow direction is consistent with simulation result as shown in Fig.3.

This experiment also demonstrated that electron pressure profiles are comparable for different gas puff cases, and that T_e at HFS SOL and T_i (measured at the LFS plasma top) decrease with the increase in n_e at the HFS SOL, in particular, at the outer flux surfaces. As a

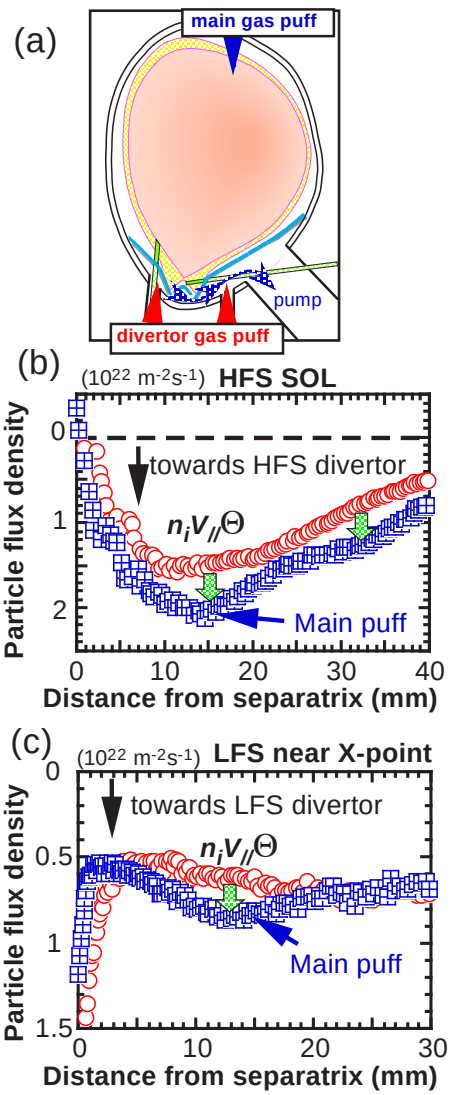

FIG. 8. (a) Locations of main puff and divertor puff. Poloidal components of parallel flux (b) at HFS, and (c) at LFS, are compared at the same n_e.

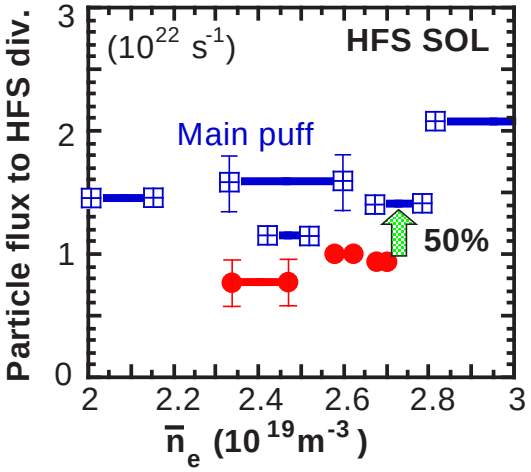

FIG. 9. Total parallel particle fluxes towards HFS divertor. Horizontal bars show increment of n_e during gas puffing.

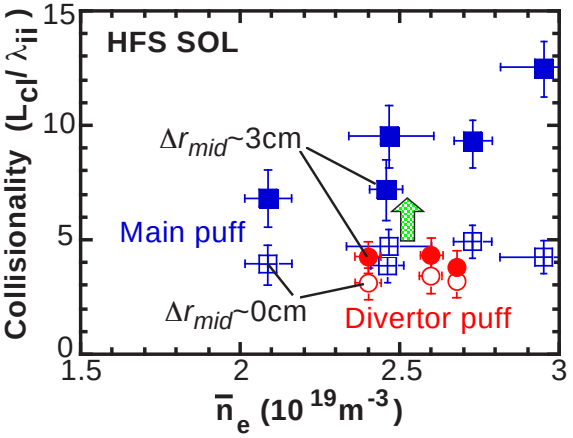

FIG. 10. Ion collisionalities at separatrix and outer flux surfaces (r_{mid}~3cm) in HFS .

result, electron and ion collisionalities, ν_e^* and ν_i^*, are increased largely at the outer flux surfaces of HFS SOL for the main puff case. Figure 10 shows that ν_i^* is enhanced by the factor of 2-3 at r_{mid} =3 cm, while an increase in ν_i^* near the separatrix is small. Values of ν_i^* (~3-5) at LFS (r_{mid} =0 and 3 cm) are comparable. A friction force on the impurity flux is enhanced by the increases in ν_i^* and M, which would overcome the thermal force (producing impurity flux towards the main plasma). Z_{eff} (the main contribution of carbon) is reduced to 1.3 during the strong main puff cases, comparing to 1.4 for the divertor gas puff. This result suggests that the impurity reduction in the main plasma is caused by enhancement of the SOL flow at HFS.

6. Summary and Conclusions

Measurements of the SOL flow both at the HFS and LFS of the JT-60U tokamak, and UEDGE simulation revealed the SOL flow pattern and effects of the plasma drifts on the SOL flow. Drift flow was dominant near the separatrix, which contributes up to 50% (HFS) and 80% (LFS) to net particle transport at relatively low density. At the same time, E_rxB drift flow in the private flux region was found to be comparable to the net particle flux towards the HFS divertor, which produces the HFS-enhanced asymmetry in the divertor ion flux under the attached divertor condition (for ion ∇B drift direction towards the divertor).

A strong gas puff from the main plasma top increased the SOL flow, in particular, at HFS by the factor of 1.5-2 under the attached divertor condition. At the same time, ν_i^* and ν_e^* increased in particular at the outer flux surfaces. Increments of both M and ν_i^* at HFS SOL enhance the friction force on impurity flux, resulting in reduction of Z_{eff}.

In a tokamak reactor such as ITER, drift effects in the particle flux transport would be expected since collisionality of the SOL plasma is relatively low. At the same time, E_rxB drift flow in the private region will exist, producing in-out asymmetry in divertor particle flux. Particle flux towards the divertor will be influenced by these drifts, and the design work including the drift effects will be useful to optimize the divertor and pump geometries.

References

[1] LOARTE, A., et al., Proc. 20th Eur. Conf. on Contr. Fusion and Plasma Physics (EPS, Lisboa) **17C** (1993) 555.
[2] PITCHER, C.S., et al., Proc. 20th Eur. Conf. on Contr. Fusion and Plasma Physics (EPS, Lisboa) **17C** (1993) 291.
[3] LaBOMBARD, B., et al.,J. Nucl. Mater. **241-243** (1997) 149.
[4] ASAKURA, N. et al., Nucl. Fusion **39** (1999) 1983.
[5] CHANKIN, A.V., STANGEBY, P.C., Plasma Phys. Control. Fusion **36** (1994) 1485.
[6] ASAKURA, N., et al., Phys. Rev. Lett. **84** (2000) 3093.
[7] ROGNLIEN, T.D., PORTER, G.D., RYUTOV, D.D., J. Nucl. Mater. **266-269** (1999) 654.
[8] BOEDO, J.A., et al., Phys. Plasma **7** (2000) 1075.
[9] HUTCHINSON, I.H., Phys. Rev. **A 37** (1988) 4358.
[10] ASAKURA, N., et al., Plasma Phys. Control. Fusion **44** (2002) 2101.
[11] PORTER, G.D., et al., Phys. Plasma **7** (2000) 3663.
[12] PORTER, G.D., et al., "Simulation of the effect of plasma flows in DIII-D, JET, and JT-60U" to be published in J. Nucl. Mater. (2003).
[13] ASAKURA, N., et al., "Plasma flow measurement in high- and low-field-side SOL and influence on the divertor plasma in JT-60U tokamak" to be published in J. Nucl. Mater. (2003).
[14] MAHDAVI, M.A., et al., J. Nucl. Mater. **220-222** (1995) 13.
[15] HOSOGANE, N., et al., J. Nucl. Mater. **266-269** (1999) 296.